Available online at www.sciencedirect.com

ScienceDirect

Energy Procedia 2 (2010) 143–150

Energy Procedia

www.elsevier.com/locate/procedia

E-MRS Spring meeting 2009, Symposium B

# Potential of advanced optical concepts in chalcopyrite-based solar cells

Benjamin Lipovšek*, Janez Krč, Marko Topič

*University of Ljubljana, Faculty of Electrical Engineering, Tržaška 25, 1000 Ljubljana, Slovenia*

Received 1 June 2009; received in revised form 1 December 2009; accepted 20 December 2009

**Abstract**

The potential of three advanced optical concepts in chalcopyrite-based solar cells is investigated by means of simulations with realistic optical and electrical parameters of state-of-the-art CGS and CIGS cells. First, a monolithically stacked tandem CGS/CIGS structure is analysed, achieving efficiencies up to 20.3 % under standard test conditions. Then, in order to reduce the effects of the parasitic sub-bandgap absorption, a wavelength-selective intermediate reflector is incorporated in the tandem, leading to efficiencies up to 20.8 %. Finally, the concept of spectrum splitting is tested in a hybrid four-terminal configuration of dislocated CGS and CIGS cells, and efficiencies up to 22.5 % are simulated. To indicate further possible improvements, all three concepts are also tested in optically and electrically idealised CGS/CIGS structures, indicating the potential of efficiencies up to 28 %.



Keywords: Chalcopyrite tandem solar cells; Advanced optical concepts; Optical and electrical modelling;

* Corresponding author. Tel.: +386-1-4768-321; fax: +386-1-4264-630.
*E-mail address*: benjamin.lipovsek@fe.uni-lj.si.

1876-6102 
doi:10.1016/j.egypro.2010.07.020

## 1. Introduction

Low-cost polycrystalline chalcopyrite materials such as $Cu(In_x,Ga_{1-x})Se_2$ – CIGS have been recognised for the potential to easily alter their bandgap, enabling better solar spectrum utilization in solar cell applications. By changing the ratio of In/Ga concentrations, bandgaps from 1.02 eV for $CuInSe_2$ (CIS) up to 1.68 eV for $CuGaSe_2$ (CGS) can be achieved [1]. This bandgap alteration ability makes them perfect candidates not only for thin-film single-junction devices but also for tandem and other advanced optical concepts of solar cells. Tandems generally consist of the top high-bandgap cell, which absorbs the short-wavelength (high-energy) part of the spectrum, and the bottom low-bandgap cell absorbing the rest. Thus, a much more efficient harvesting of the solar spectrum can be achieved since the photo-generated carriers normally carry less excess energy. Under standard AM1.5 illumination conditions, the optimal top and bottom cell bandgaps of 1.71 eV and 1.14 eV have been determined [2], respectively, which is almost ideally within the range of the CIGS bandgaps.

In this work, the potential of three advanced concepts in the design of chalcopyrite-based solar cells, aiming for higher conversion efficiency, is investigated by means of optical and electrical modelling. First, the potential of monolithically stacked CGS top cell and CIGS bottom cell in a tandem configuration is investigated. The effects of the top CGS thickness and the bottom CIGS bandgap are analysed, and their optimal values for the highest conversion efficiency are determined. Then, in order to boost the performance of the tandem, a wavelength-selective intermediate reflector (WSIR) is inserted between the top and the bottom cell to eliminate the effects of the sub-bandgap absorption in the CGS cell. As the third case, the concept of spectrum splitting applied in a hybrid four-terminal configuration of CGS and CIGS cells is investigated. Primarily, realistic optical and electrical parameters of current state-of-the-art CGS and CIGS cells are used in the simulations. However, to indicate the potential for further improvements of the concepts, the simulations are also carried out for the idealised parameters. The results of the calculated conversion efficiencies indicate that by applying the advanced concepts, efficiencies up to 23 % can be achieved for the case of realistic parameters of the cells, and more than 28 % for the case of optically and electrically improved CGS and CIGS cells.

## 2. Simulation method

The one-dimensional semi-coherent optical simulator SunShine [3] is employed to determine the external quantum efficiency (*QE*) and the short-circuit current density ($J_{SC}$) of the investigated solar cells. For this determination, a detailed optical analysis combined with a simplified (but justified) electrical analysis is used. As the first step, the external *QE* is equalised to the calculated absorptance in the CGS or CIGS layer. Then, the effects of the non-ideal charge carrier extraction especially in the CGS absorber are included following the *QE* data of the state-of-the-art CGS and CIGS cells. The $J_{SC}$ is calculated from such determined *QE* by applying the AM1.5 solar spectrum. In the simulations, realistic complex refractive indices of the layers (including the sub-bandgap absorption in CGS and CIGS layers [4] and the free carrier absorption in transparent conductive oxide – TCO layers) are taken into account.

The conversion efficiencies (*Eff*) of the investigated structures are determined from the simulated $J_{SC}$ by applying the standard diode model and then calculating the open-circuit voltage ($V_{OC}$) and the fill factor (*FF*) from the *J-V* characteristics. For these calculations, realistic electrical parameters of the chalcopyrite absorbers (i.e. the bandgap ($E_G$), the saturation current density ($J_0$), and the diode ideality factor ($A$)) are assumed, which are extracted from the latest reported state-of-the-art cells: (i) CGS: $E_G$ = 1.68 eV, $J_0 = 7 \cdot 10^{-7}$ mA/cm$^2$, $A$ = 2.1 [5]; and (ii) CIGS: $E_G$ = 1.18 eV, $J_0 = 2.1 \cdot 10^{-9}$ mA/cm$^2$, $A$ = 1.14 [6]. The saturation current density of CIGS absorbers with bandgaps other than 1.18 eV is extrapolated according to Eq. 1 [4].

$$J_0 = J_{00} \cdot \exp\left(-E_G / \left(A \cdot k \cdot T\right)\right) \tag{1}$$

## 3. Results and discussion

The potential of three advanced concepts of chalcopyrite-based solar cells is investigated by means of simulations:

(a) the monolithically stacked CGS/CIGS tandem structure (Fig. 1a),

(b) the CGS/CIGS tandem enhanced with a WSIR (Fig. 1b),

(c) the concept of spectrum splitting applied in a hybrid four-terminal configuration of dislocated CGS and CIGS solar cells (Fig. 1c).

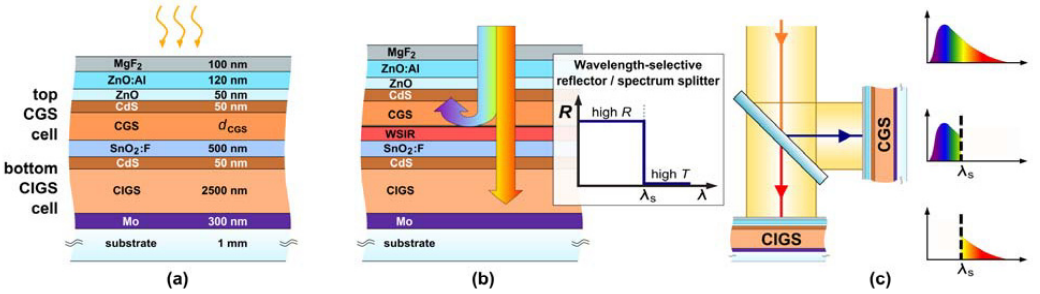


Figure 1: The analysed concepts of chalcopyrite-based solar cells: (a) a monolithically stacked tandem, (b) a monolithically stacked tandem with a WSIR, and (c) the concept of spectrum splitting applied in a hybrid four-terminal configuration of dislocated cells.

### *3.1. Monolithically stacked CGS/CIGS tandem solar cells*

In a monolithically stacked CGS/CIGS tandem, the top CGS and the bottom CIGS cells are optically and electrically connected with a layer of $SnO_2$:F transparent conductive oxide (TCO). A thin Mo layer between the CGS and the $SnO_2$:F for improving the ohmic contact of the interface was not considered in the simulations. The transparent front contact is realised as a combination of the intrinsic ZnO and *n*-doped ZnO:Al TCO. In order to reduce the reflection losses, a thin layer of $MgF_2$ antireflective coating is deposited on top of the ZnO:Al TCO layer. The thicknesses of the individual layers are given in Fig. 1a.

The bandgap of the top CGS absorber was set to 1.68 eV, which is close to the theoretically optimal value for the tandems [2]. Two parameters were varied and optimised in the analysis: (i) the thickness of the top CGS absorber ($d_{CGS}$), and (ii) the bandgap of the bottom CIGS absorber ($E_{G,\,CIGS}$). The effects of the $d_{CGS}$ on the *QE* are presented in Fig. 2 for two selected thicknesses and for $E_{G,\,CIGS}$ = 1.15 eV. For the case of a thick CGS absorber (1700 nm) the $J_{SC,\,CGS}$ = 17.5 mA/cm$^2$ is determined for the top cell. However, due to the high $d_{CGS}$, the pronounced parasitic sub-bandgap absorption in the CGS layer severely hinders the transparency of the top cell in the long-wavelength region ($\lambda$ > 740 nm). Thus, the $J_{SC}$ in the bottom CIGS cell is limited ($J_{SC,\,CIGS}$ = 14.1 mA/cm$^2$). The simulation results show that in this case, 5.1 mA/cm$^2$ of the potential $J_{SC}$ is lost due to the sub-bandgap absorption in the top CGS absorber. Therefore, in order to assure better current matching, the $d_{CGS}$ needs to be optimised. The optimisation results indicate that if the $d_{CGS}$ is reduced to 1050 nm, a lower $J_{SC,\,CGS}$ = 16.4 mA/cm$^2$ and a less pronounced sub-bandgap absorption are achieved. In this case, only 3.3 mA/cm$^2$ of the potential $J_{SC}$ is lost due to the sub-bandgap absorption in the top CGS cell, while the $J_{SC,\,CIGS}$ is increased to 16.3 mA/cm$^2$. Comparing the $J_{SC,\,CGS}$ and $J_{SC,\,CIGS}$, it can be observed that now the top and the bottom cell are current-matched, which is of primary importance for efficient tandems. Thus, the thickness $d_{CGS}$ of 1050 nm was indicated as the optimal value for this tandem.

The bandgap of the bottom CIGS absorber, on the other hand, affects both the $J_{SC}$ and the $V_{OC}$ of the cell, according to the diode model. Higher $E_{G,\,CIGS}$ results in a higher $V_{OC}$, but lower $J_{SC,\,CIGS}$. Therefore, since both the $d_{CGS}$ and the $E_{G,\,CIGS}$ affect the performance of the tandem, they need to be optimised simultaneously, as presented in the following.

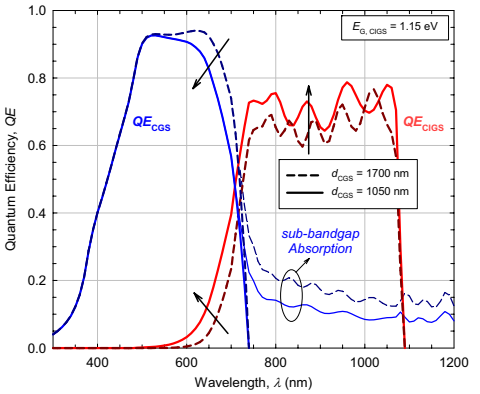


Figure 2: The simulated *QE* of CGS/CIGS tandems with different top CGS absorber thicknesses. The effects of thinning down the CGS absorber are indicated by arrows.

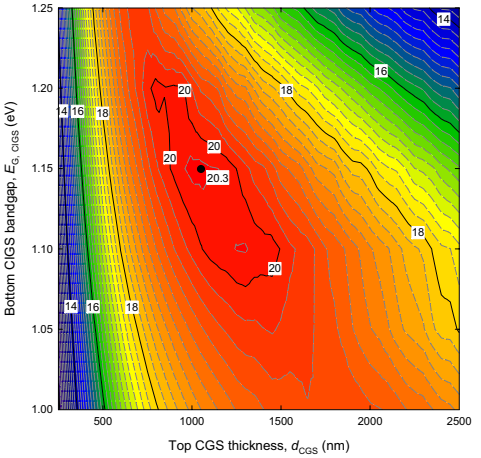


Figure 3: The calculated conversion efficiencies of CGS/CIGS tandems for different $d_{CGS}$ / $E_{G,\ CIGS}$ combinations. The maximal efficiency of 20.3 % can be achieved, considering the realistic state-of-the-art parameters for CGS and CIGS cell.

In order to determine the optimal values of the $d_{CGS}$ and $E_{G,\ CIGS}$, rendering the highest *Eff* of the tandem cell, an extensive set of simulations was carried out in which both parameters were varied from 100 – 2500 nm and from 1.00 – 1.25 eV, respectively. The results presented in Fig. 3 indicate that by using the realistic optical and electrical parameters of the CGS and the CIGS cell, the maximal tandem efficiency of 20.3 % can be achieved (see also Table 1). Furthermore, it can also be observed that the area with high efficiencies (*Eff* > 20 %) is localised tightly around the optimal values, which are $d_{CGS} \approx 1050$ nm and $E_{G,\ CIGS} \approx 1.15$ eV.

To indicate potential further improvements in the tandem performance, an optically and electrically idealised CGS cell was assumed in the CGS/CIGS tandem. In particular, two cases of idealisation were assumed: first, the sub-bandgap absorption in the CGS absorber was excluded, and second, the electrical parameters of the state-of-the-art CIGS cell were employed to the CGS cell. The results that are summarised in Table 1 show that in the case of an idealised CGS cell, a much higher conversion efficiency of the tandem (*Eff* = 27.5 %) could be achieved. Thus, improving the electrical and optical performance of the top CGS cell presents a crucial step for highly efficient tandems. Along with this, advanced concepts that minimise the effects of the sub-bandgap absorption need to be developed. Two of them are analysed in the following.

Table 1: Maximal achieved conversion efficiencies and optimal parameters for different advanced concepts.

| | Simulations based on realistic parameters | Simulations based on idealised CGS parameters |
|---|---|---|
| Monolithic CGS/CIGS tandem | $d_{CGS}$ = 1050 nm<br>$E_{G, CIGS}$ = 1.15 eV<br>***Eff* = 20.3 %** | $d_{CGS}$ = 2500 nm<br>$E_{G, CIGS}$ = 1.10 eV<br>***Eff* = 27.5 %** |
| Monolithic CGS/CIGS tandem with a WSIR | $d_{CGS}$ = 800 nm<br>$E_{G, CIGS}$ = 1.15 eV<br>$\lambda_S$ = 680 nm<br>***Eff* = 20.8 %** | $d_{CGS}$ = 2500 nm<br>$E_{G, CIGS}$ = 1.10 eV<br>$\lambda_S$ = 710 nm<br>***Eff* = 28.0 %** |
| The concept of spectrum splitting and dislocated cells | $d_{CGS}$ = 2500 nm<br>$E_{G, CIGS}$ = 1.10 eV<br>$\lambda_S$ = 710 nm<br>***Eff* = 22.5 %** | $d_{CGS}$ = 2500 nm<br>$E_{G, CIGS}$ = 1.10 eV<br>$\lambda_S$ = 720 nm<br>***Eff* = 28.1 %** |

### *3.2. CGS/CIGS tandem solar cells with a wavelength-selective intermediate reflector (WSIR)*

In order to reduce the limiting effects of the realistic sub-bandgap absorption in the CGS cell, we introduce a wavelength-selective intermediate reflector (WSIR), which is inserted between the $SnO_2$:F TCO and the top CGS cell of the CGS/CIGS tandem (Fig. 1b). The function of the WSIR is to: (i) efficiently reflect the short-wavelength (high-energy) part of the spectrum back into the top CGS cell, and (ii) efficiently transmit the long-wavelength (low-energy) part into the bottom CIGS cell. Due to the enhanced reflectivity properties in the short-wavelength region and thus an increased absorption in the top cell, the CGS absorber can be thinner and therefore the optical losses related to the sub-bandgap absorption can be minimised. The desired reflectance characteristics $R(\lambda)$ of the WSIR (see inset in Fig. 1b) can be realised, for example, by photonic-crystal-like structures in the role of distributed Bragg reflectors, which also need to be conductive in this case [7]. In the reflectance characteristics, $\lambda_S$ represents the threshold wavelength of the WSIR. In our simulations, an ideal WSIR was applied ($R$ = 1 for $\lambda < \lambda_S$; $T$ = 1 for $\lambda > \lambda_S$).

The effects of the WSIR on the *QE* of the CGS/CIGS tandem are presented in Fig. 4. In the region of $\lambda$ = 500 – 700 nm, the WSIR ($\lambda_S$ = 680 nm) significantly enhances the *QE* of the top CGS cell ($d_{CGS}$ = 800 nm) compared to the tandem without the WSIR. Furthermore, if the optical combination CGS/WSIR/TCO renders lower reflectance than the CGS/TCO interface for $\lambda > \lambda_S$, the *QE* of the bottom CIGS cell can be enhanced as well as seen in the figure.

The optimal $d_{CGS}$ and $E_{G, CIGS}$ of the tandem with the optimal WSIR ($\lambda_S$ = 680 nm) can be determined from the mapping presented in Fig. 5. Here, the highest *Eff* of 20.8 % is obtained for the cells with the realistic optical and electrical parameters. Comparing to Fig. 3, it can be observed that the area with high tandem efficiencies is now much wider, which allows for greater freedom in the design with respect to $d_{CGS}$ and $E_{G, CIGS}$. The optimal $d_{CGS}$ and $E_{G, CIGS}$ are 800 nm and 1.15 eV, respectively. Furthermore, as a result of the enhanced active bandgap absorption in the CGS layer, the optimal $d_{CGS}$ is shifted towards lower values (≈ 800 nm), which would reflect in a lower material consumption. Finally, the optimal threshold wavelength of the WSIR must also be carefully selected to assure the optimal distribution of the spectrum between the top and the bottom cell, thus assuring a high level of $J_{SC}$ matching and high *Eff* of the cell. In our case, the optimal $\lambda_S$ = 680 nm was determined.

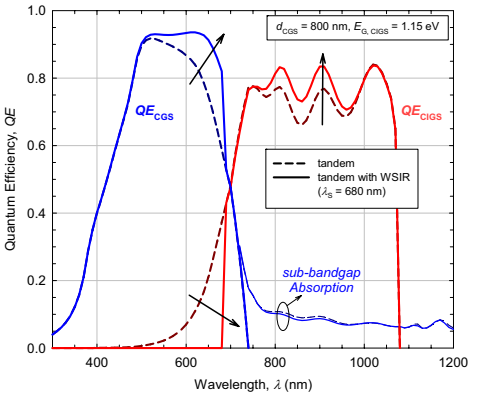


Figure 4: The effects of the wavelength-selective intermediate reflector ($\lambda_S$ = 680 nm) on the *QE* of a CGS/CIGS tandem.

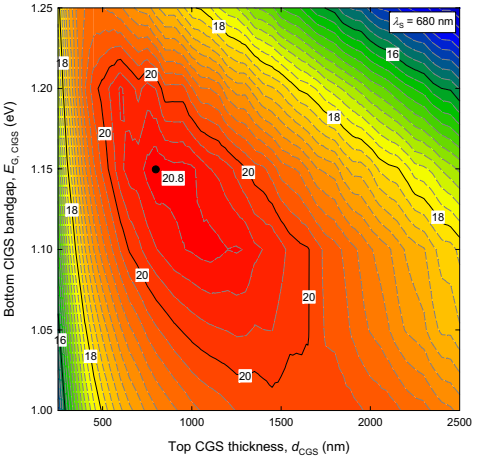


Figure 5: The calculated conversion efficiencies of the WSIR-upgraded CGS/CIGS tandem for different $d_{CGS}$ / $E_{G, CIGS}$ combinations. The maximal efficiency of 20.8 % can be achieved considering realistic parameters of the CGS cell.

The implementation of a WSIR was also tested for the case of a tandem with an idealised CGS cell, where the highest efficiency of 28.0 % was indicated for $d_{CGS}$ = 2500 nm and $E_{G, CIGS}$ = 1.10 eV. (see Table 1).

### *3.3. The concept of spectrum splitting in a hybrid configuration of dislocated CGS and CIGS solar cells*

The negative effects of the sub-bangap absorption can be completely eliminated by the concept of spectrum splitting (Fig. 1c). Instead of the vertical monolithic integration, the CGS and CIGS cells are constructed separately and connected in a hybrid four-terminal configuration. A wavelength-selective spectrum splitter (could be realised with dichroic mirrors [8]) with the characteristic split point $\lambda_S$ is employed to physically split the incident solar spectrum into two parts. These two parts are then distributed between the two chalcopyrite-based cells. The CGS cell is illuminated by the short-wavelength ($\lambda < \lambda_S$) part, and the CIGS by the long-wavelength ($\lambda > \lambda_S$) part of the spectrum. The role of the spectrum splitter here is similar to the role of the WSIR in the previous concept.

Since the parasitic sub-bandgap absorption in the CGS absorber does no longer affect the photocurrent generation in the CIGS cell, the $d_{CGS}$ can be sufficiently thick, which results in a higher $J_{SC, CGS}$. On the other hand, the CIGS bandgap and the spectrum split point $\lambda_S$ still need to be optimised in order to achieve good current matching and high total conversion efficiencies ($Eff = Eff_{CGS} + Eff_{CIGS}$). The optimisation results for different $\lambda_S$ and $E_{G, CIGS}$ are plotted in Fig. 6. The results indicate that the carefully selected $\lambda_S$ is indeed crucial for a high *Eff* and should not deviate from the optimal value (deviations should be less than 20 nm). The $E_{G, CIGS}$, on the other hand, allows for more freedom since similar results are rendered for CIGS bandgaps between 1.10 – 1.15 eV. The maximal efficiency of 22.5 % can be achieved for $E_{G, CIGS}$ = 1.10 eV and $\lambda_S$ = 710 nm, considering the realistic optical and electrical parameters of the cells (see Table 1). For the case of the idealised CGS cell, on the other hand, the maximal combined efficiency of 28.1 % was determined. Here, the enhancement is related to the improved electrical parameters of CGS.

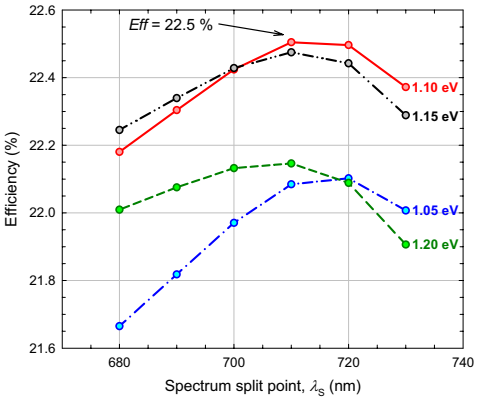


Figure 6: The effects of the spectrum split point and the CIGS bandgap on the total conversion efficiency of the cells connected in a hybrid four-terminal configuration.

## 4. Conclusions

The potential of three advanced optical concepts in the design of chalcopyrite-based solar cells was investigated by means of numerical simulations. In the simulations, realistic optical and electrical parameters of the state-of-the-art CGS and CIGS cells were assumed. The results show that the efficiency of the monolithically stacked CGS/CIGS tandem is severely limited by the parasitic sub-bandgap absorption in the top CGS absorber, which calls for a careful optimisation of the top CGS thickness and the bottom CIGS bandgap. In the optimal case, a conversion efficiency of 20.3 % can be achieved, considering the realistic parameters. By means of the wavelength-selective intermediate reflector inserted between the two cells of the tandem, however, the effects of the sub-bandgap absorption can be reduced, and the $J_{SC}$ generation in the CGS cell increased. Thus, a conversion efficiency of 20.8 % can be achieved, while the CGS absorber thickness can be reduced substantially. Finally, the concept of spectrum splitting was tested in a hybrid four-terminal configuration of dislocated CIGS and CGS cells. For the case of optimal spectrum distribution, a conversion efficiency of 22.5 % can be achieved. However, to further boost the efficiency of chalcopyrite-based cells, the electrical performance of the CIGS and especially the CGS absorber will also need to be further enhanced. Thus, it could be possible to reach efficiencies up to 28 %.

## References

[1] T. Dullweber et al., "Study of the effect of gallium grading in Cu(In,Ga)Se2", *Thin Solid Films 361-362* (2000), pp. 478-481.
[2] T. J. Coutts et al., "Critical issues in the design of polycrystalline, thin-film tandem solar cells", *Progress in Photovoltaics: Research and Applications 11* (2003), pp. 359-375.
[3] J. Krč, F. Smole, M. Topič, "Analysis of light scattering in amorphous Si:H solar cells by a one-dimensional semi-coherent optical model", *Progress in Photovoltaics: Research and Applications 11* (2003), pp. 15-26.
[4] M. Schmid, R. Klenk, M. Ch. Lux-Steiner, J. Krč, M. Topič, "Optical modeling of chalcopyrite-based tandems considering realistic layer properties", *Applied Physics Letters 94/5* (2009), pp. 1-3.
[5] D. L. Young et al., "Improved performance in ZnO/CdS/CuGaSe2 thin-film solar cells", *Progress in Photovoltaics: Research and Applications 11* (2003), pp. 535-541.
[6] I. Repins et al., "19.9%-efficienct ZnO/CdS/CuInGaSe2 solar cell with 81.2% fill factor", *Progress in Photovoltaics: Research and Applications 16* (2008), pp. 235-239.
[7] J. Krč, M. Zeman, S. L. Luxembourg, M. Topič, "Modulated photonic-crystal structures as broadband back reflectors in thin-film solar cells", *Applied Physics Letters 94/15* (2009), pp. 1-3.
[8] W. Chen, P. Gu, "Design of non-polarizing color splitting filters used for projection display system", *Displays 26* (2005), pp. 65-70.

[9] M. Schmid, R. Klenk, M. Ch. Lux-Steiner, "Quantitative analysis of cell transparency and its implications for the design of chalcopyrite-based tandems", *Solar Energy Materials & Solar Cells 93* (2009), pp. 874-878.
[10] T. Nakada, Y. Hirabayashi, T. Tokado, D. Ohmori, "Cu(In1-1,Gax)Se2 thin film solar cells using transparent conducting oxide back contacts for bifacial and tandem solar cells", *Journal of Applied Physics 41* (2002), pp. 209-211.
[11] M. Gloeckler, J. R. Sites, "Efficiency limitations for wide-band-gap chalcopyrite solar cells", *Thin Solid Films 480-481* (2005), pp. 241-245.
[12] J. AbuShama et al., "Improved performance in CuInSe2 and surface-modified CuGaSe2 solar cells", *Conference record of the 31st IEEE Photovoltaics Specialists Conference and Exhibition* (2005), pp. 299-302.